J Mater Sci (2007) 42:7141–7146
DOI 10.1007/s10853-007-1681-z

Preparation of rutile (TiO_2) nanostructured materials at low temperature from $TiCl_4$ aqueous solution

Ru-Fen Chen · Lei Zhang · Yu Wei · Deng-Lu Hou

Received: 4 October 2006 / Accepted: 9 March 2007 / Published online: 9 June 2007

Abstract The synthesis of rutile (TiO_2) nanostructured materials at low temperature from $TiCl_4$ aqueous solution was described. TiO_2 coatings on polystyrene (PS) particles were prepared by layer-by-layer assembly technique. The samples were characterized by DTA-TG, SEM, XPS, TEM and XRD techniques. The experimental results showed that pure rutile-TiO_2 coatings with nanocrystal structure were synthesized at 100 °C. On the surface of PS particles, sphere-type TiO_2 coatings exhibited uniform shape and a narrow size distribution. The amount of TO_2 (wt%) and shell thickness of particles increased with the adding of coating layers. Hollow TiO_2 spheres were obtained by calcination at 450 °C. TiO_2/PS with 2 coating layers showed higher degradation rate. The photocatalytic activity of hollow TiO_2 spheres was higher than that of TiO_2/PS.

Introduction

Nanosized titania is the most effective photocatalyst and has been widely applied in purification of water and air [1, 2]. Titania exists in three main crystallographic forms: anatase, rutile and brookite phases. In photocatalysis research, anatase titania is usually considered to be more active than rutile crystalline [3, 4]. However, rutile TiO_2 has some advantages over anatase such as chemical stability, refractive index and chemical inertness [5]. In addition, rutile phase has a narrower band gap (3.0 eV) than anatase phase (3.2 eV). Consequently, rutile TiO_2 should be easily shifted to the visible light region by suitable modifications [4, 6]. Qiujing Yang et al. [7] prepared highly active sulfate-promoted rutile TiO_2 that could be efficiently operated in the visible light region by an in site sulfation method. Therefore, rutile TiO_2 should be more suitable for practical use in the field of environmental cleanup.

Nanocrystalline rutile powders are difficult to obtain at low temperature. Heat treatment is usually required to achieve rutile phase via a phase transition from anatase to rutile, which usually takes place at around 600–800 °C. However, calcinations unavoidably lead to aggregation and growth of the nanocrystallites [8–10]. Recent reports suggested that hydrothermal method and hydrolysis of $TiCl_4$ aqueous solution could form rutile nanocrystals at lower temperatures [1, 11–13]. But the synthesis of well-shaped rutile nanocrystals via hydrolysis in solution was much more difficult than anatase nanocrystals [8, 14].

In addition, aggregation and difficulty in recovering often limited the application of nanosize TiO_2 powder in practice. To solve the problem, many supported photocatalysts of TiO_2 and hollow TiO_2 spheres were investigated [6, 15, 16]. But, in general, those core-shell nanostructured TiO_2 prepared at low temperature were anatase structure [17–19]. Therefore, development of a simple method for preparation of pure rutile (TiO_2) nanostructured material at low temperature is of significant.

Herein, we describe a simple aqueous solution route to synthesize rutile (TiO_2) nanostructured materials at low temperature (100 °C) from $TiCl_4$ aqueous solution. Using anionic surfactant (sodium dodecyl sulfate) as self-assembled monolayers (SAMs), nanostructured TiO_2/PS particles

R.-F. Chen · L. Zhang · Y. Wei (✉)
College of Chemistry and Material Science, Hebei Normal University, Shijiazhuang, Hebei 050016, China
e-mail: weiyu@mail.hebtu.edu.cn

D.-L. Hou
College of Physics Science and Information Engineering, Hebei Normal University, Shijiazhuang, Hebei 050016, China

are prepared by layer-by-layer assembly technique. Hollow TiO_2 sphere with nanocrystal grain structure are obtained by a controllable way. The structure, surface characterization and photocatalytic activity of samples are investigated in this study.

Experimental

Materials

Titanium tetrochloride ($TiCl_4$), hydrochloric acid (HCl), ammonium hydroxide (NH_3 28%), sodium dodecyl sulfate (SDS) and PS are purchased from Tianjin Chemical Reagent Company with the purity of 99%. All chemicals are used as received without further purification. The solvent used for the reaction is distilled water.

Preparation of TiO_2/PS particles and hollow TiO_2 spheres

As carrier, PS particles (1 g, particle size about 0.2 mm) were cleaned sequentially with aqueous ammonium hydroxide (NH_3 28%, 3 mol/L, 80 mL), HCl (3 mol/L, 80 mL), ethanol (20 mL) and distilled water (50 mL). The SAMs were then deposited by immersing the PS carrier (1 g) into the solution of SDS (5 mmol/L, 100 mL) for 2 h. After being rinsed (with distilled water) and dried in oven (100 °C), the carriers with SAMs were immersed in the TiO_2 colloid dispersions, which were prepared from titanium tetrochloride (0.5 mol/L, 100 mL) and hydrochloric acid (4 mol/L, 100 mL). Then, this mixture in a 250 mL beaker was heated with water bath at 80 °C for 2 h (TiO_2 colloidal particles carry a position surface at $pH < 6$, electrostatic interactions between the TiO_2 colloidal particles and anionic surfactant). Then they were aged for 24 h at room temperature. After being rinsed with distilled water and dried, the monolayer coated TiO_2 particles were obtained. In an attempt to increase the thickness of TiO_2, multi-layer coatings were also prepared with the same method as the monolayer by layer-by-layer assembly technique except for altering the concentration of SDS (7 mmol/L, 100 mL) to form micelle. Repeating cycles of TiO_2 and SAMs were illustrated in Fig. 1. TiO_2/PS particles with multi-layer coatings were heated at the rate of 40 °C /min from 100 °C to 450 °C. And then, hollow TiO_2 spheres were obtained after calcination at 450 °C.

Photocatalytic reaction system

TiO_2/PS and hollow TiO_2 spheres were applied to the reaction of methyl orange degradation. The TiO_2/PS particles (1 g) and their hollow TiO_2 spheres were immersed in the methyl orange solution (1 mg/L).The solution was stirred while the sample was irradiated by high-pressure mercury lamp (160 W) light. The sample was separated after irradiation. The concentration of methyl orange was determined with a spectrophotometer by measuring the absorption at 462 nm, because aqueous solution of methyl orange showed the intense band at approximately 462 nm.

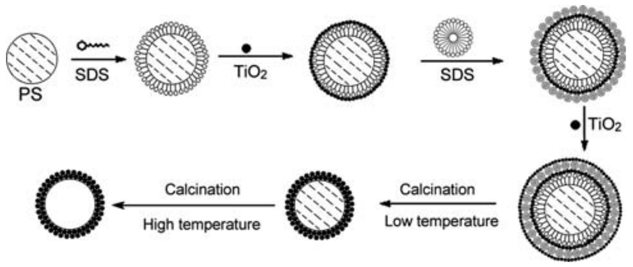

Fig. 1 Schematic illustration of nanostructured TiO_2/PS by layer-by-layer assembly technique

Characterization

The structures of samples were characterized by X-ray diffraction patterns (Bruker Axs D8 ADVACE), recorded on a Rigaku/Rotaflex/RINT rotating anode diffractometer using Cu Kα radiation. Thermogravimetric (TG) and Differential Thermal Analysis (DTA) experiments were performed using a Rigaku-TG8101D thermal analyzer at a scan rate of 10 °C/min. The morphologies of the samples were obtained by a transmission electron microscopy (TEM, Hitachi H-7500) and a scanning electron microscopy (SEM Japan S-570). The compositions of coated samples were analyzed by X-ray photoelectron spectroscopy (XPS) using a VG Scientific ESCALABII electron spectrometer. A Mg Kα X-ray source ($h\gamma = 1253.6$ ev) was used. The base pressure in the spectrometer chamber was 1×10^{-8} Pa. The analyzer was operated at 50 ev for survey spectra. Spectroscopic analyses of TiO_2/ SiO_2 were performed by using a UV-visible spectrophotometer (type UV 160 A).

Results and discussion

Thermal Analysis

The thermogravimetric and thermal analysis of PS and TiO_2 / PS (4 coating layers) were carried out. We can see from Fig. 2 that there are one and three endothermic peaks in DTA curves of PS and TiO_2/PS, respectively. The endothermic peaks at 130 °C and 250 °C are attributed to the removal of water [20], and the endothermic peak at 350 °C belongs to the decomposition of the SDS and the PS particles. There are not any exothermic or endothermic peaks at high temperatures (>450 °C). Thermogravimetric analysis of TiO_2/PS can be divided into two stages. The first stage is from room temperature to about 260 °C. The second stage is from 300 to 450 °C. In the second stage, the rate of weight loss is greater, which is mainly caused by the decomposition of the PS. From the TG–DTA curves, the temperature of calcination should be performed at 450 °C if we want to get the hollow TiO_2 spheres.

Surface characterization

Figure 3 shows the XPS survey spectrum for the surface of 8 coating-layer particles calcined at 260 °C for 2 h. The XPS spectrum reveals characteristic peaks from Ti, C, and O. The photoelectron peak for Ti2p appears at a binding energy clearly, $E_b = 458.5$ eV, O1s at $E_b = 533.1$ eV, and C1s at $E_b = 284.5$ eV, respectively. In order to measure the amount of TiO_2 (wt %) on the PS particles, the TiO_2/PS particles were heated at 260 °C and 450 °C, respectively. The relative weight of TiO_2 (wt%) was estimated as follow: TiO_2 (wt%) = w_2/w_1 (where w_1 and w_2 are the weight of TiO_2/PS particles heat-treated at 260 °C and 450 °C, respectively). Figure 4 shows the relative weight of TiO_2 (wt%) with various coating layers. As is seen that, the relative weight of TiO_2 (wt%) increases with the adding of coating layers.

Figure 5 shows the scanning electron microscopy pictures of the surface sample of the uncoated PS particle (a) and the TiO_2/PS particle (4 coating layers) heat-treated at 260 °C for 2 h. From the two pictures, we can find that the surface features are different between PS particle coated with TiO_2 powders and an uncoated PS particle. As is shown from Fig. 5b, uniform TiO_2 coatings on PS have been formed and the TiO_2 coatings are an aggregation of sphere-type particles.

TiO_2/PS particles (8 coating layers) were heated from 100 °C to 450 °C. Figure 6 shows hollow spheres of TiO_2 obtained after calcinating at 450 °C. In some of them openings on the surface can be observed. The openings are probably due to the decomposition of the PS particles. By the experiment, we found that the thickness of the TiO_2 coatings is an important factor for the stability of the hollow spheres. The hollow spheres partially burst when the TiO_2 coatings were too thin. The thickness of the coatings was controlled by the number of coating layers. The optimum number of coating layers was found within the range from 6 to 10 layers. The hollow spheres of TiO_2 were ground into powders. Figure 7 displays the TEM image of TiO_2 powders, which shows clearly that the shape of TiO_2 samples is spherical and the size of TiO_2 particles is ca.

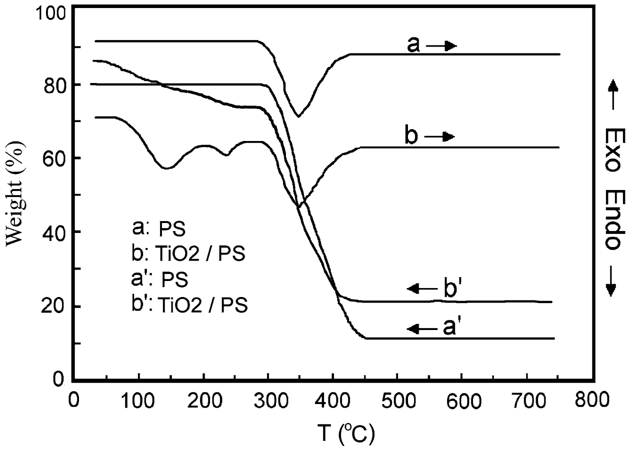

Fig. 2 DTA-TG curves of PS and TiO_2/PS

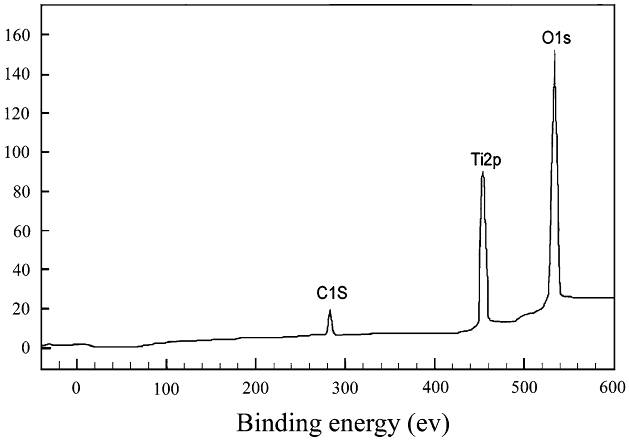

Fig. 3 XPS survey spectrum for the surface of TiO_2/PS with 8 coating layers

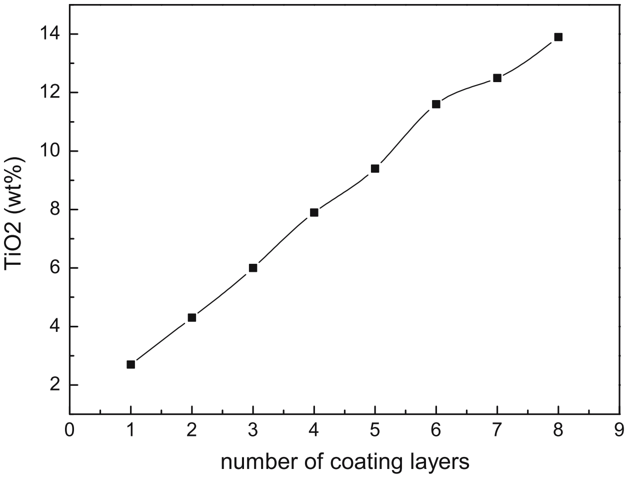

Fig. 4 Relative weight of TiO_2 with various coating layers

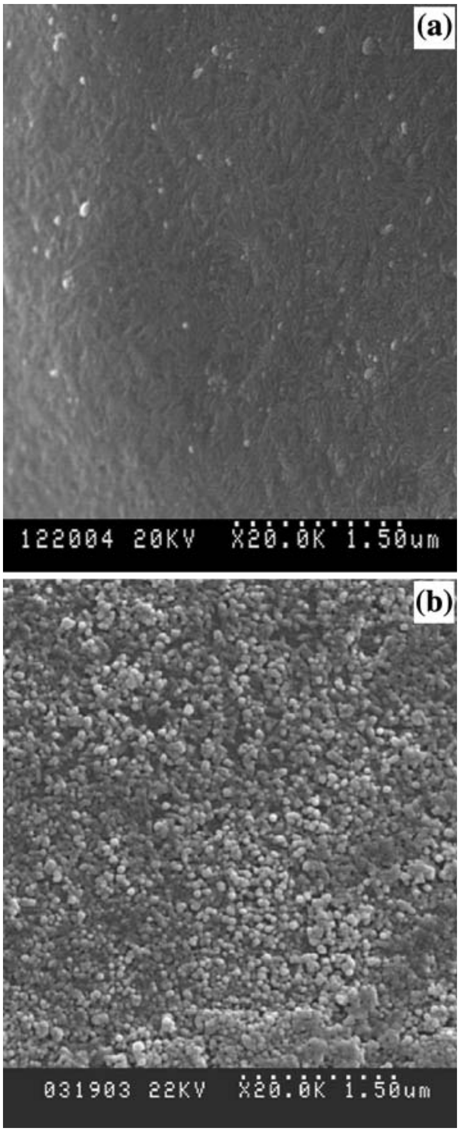

Fig. 5 Surface morphologies of uncoated PS (**a**) and TiO_2 /PS with 4 coating layers (**b**)

45 nm. Meanwhile, TiO_2 displays uniform shape and has a narrow size distribution.

XRD Study

Figure 8 shows XRD patterns of the PS and the TiO_2/PS particles (8 coating layers) calcined at different temperatures for 2 h. It is observed that the PS particle is of amorphous phase, and the shell structure appears to be composed of rutile phase TiO_2 at 100 °C. The XRD peaks of rutile phase become sharper with the increasing calcination temperature. When the TiO_2/PS particles are calcined at 450 °C, the amorphous peak of PS particles disappears because of the decomposition of the PS particles. And the TiO_2 shells always consist of the rutile phase.

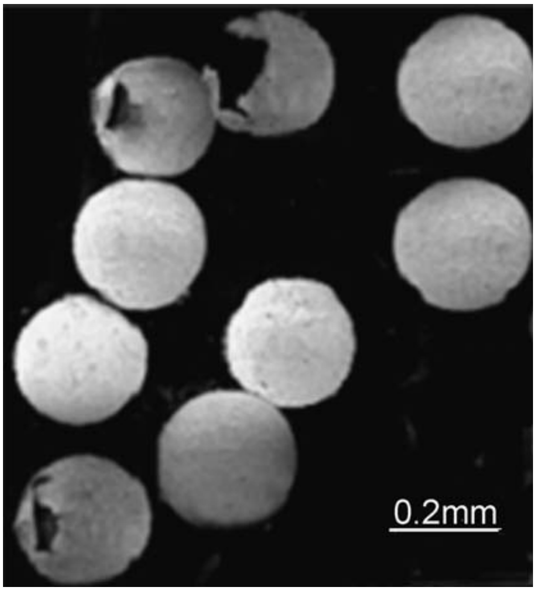

Fig. 6 SEM micrograph of the TiO_2/PS by calcination at 450 °C

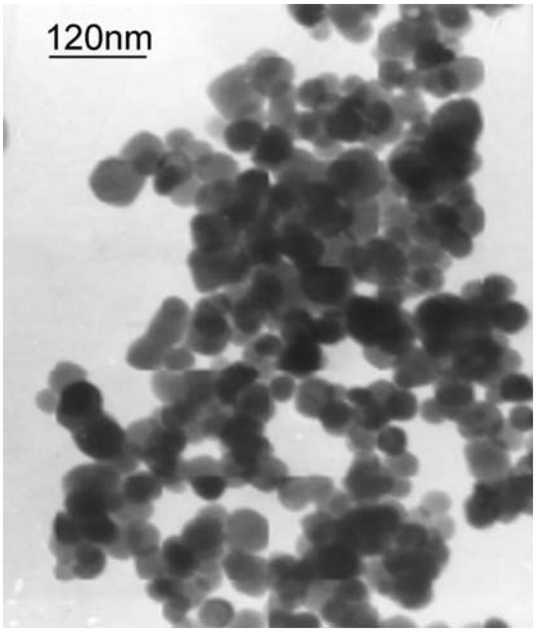

Fig. 7 TEM image of TiO_2 powders of hollow spheres by calcination at 450 °C

The formation of rutile TiO_2 at low temperature is because $TiCl_4$ solution in a strong acid condition (4 mol/L HCl) benefits the formation of rutile phase. Nannan et al. [6] reported that high concentration of H^+ suitably favored the formation of rutile while lower concentration favored the anatase one. It is well known that anatase consists of TiO_6 octahedra, which share corners and four edges with neighboring octahedral, while rutile TiO_6 octahedra share corners and two edges with neighboring octahedral [21].

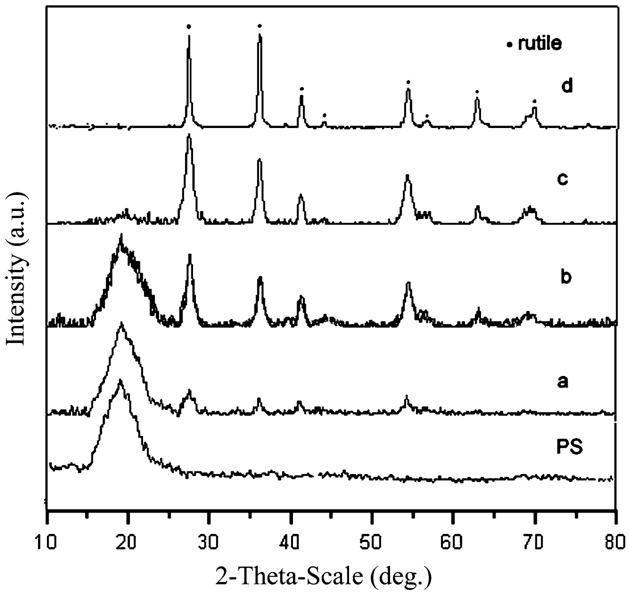

Fig. 8 XRD diagram of PS and TiO_2/PS by calcination at different temperatures: (**a**) 100 °C (**b**) 260 °C. (**c**) 450 °C. (**d**) 600 °C

Both anatase and rutile TiO_2 can grow from TiO_6 octahedra and that the phase transition proceeds by rearrangement of the octahedral [13]. In the process of peptization, there should be a competition between the two growth units of anatase and rutile. When H^+ concentration is higher in solution, more oxolation bonds among titanium atoms are broken and produced more OH groups around a single titanium atom, which facilitates the movement of the titanium atom which has been confined to its adjacent neighbors before peptization. Condensations among titania hydrates can take place among several titanium species, leading to structural rearrangement towards the formation of corner-shared octahedral chains characteristic of the rutile phase [4, 7]. Herein, H^+ in the solution rearranges the amorphous precipitate and results in crystalline rutile TiO_2. Thus, H^+ plays a catalytic role in the transformation of titania from amorphous to rutile at low temperature, which is consistent with the results of Yuanzhi Li et al. [22].

Photocatalytic activity

As photocatalyst, TiO_2/PS particles calcined at 260 °C were applied to the reaction of methyl orange solution degradation. The photocatalytic activity of TiO_2/PS was evaluated by the degradation rate of methyl orange solution. Table 1 shows the degradation rate of methyl orange by using TiO_2/PS (1–8 layers) as photocatalyst under light irradiation. The reaction time of methyl orange degradation was 5 h.

It can be seen that the TiO_2/PS particles with 2 coating layers show the highest degradation rate among all different layers samples. TiO_2/PS particles with 1 coating layer, have small amount of TiO_2, exhibit lower photocatalytic activity. On the other hand, photocatalytic chemical reaction mainly occurs on the surface of TiO_2/PS, titanium dioxide in the interior region is not easy to contact the reactant. So, the photocatalytic activity of TiO_2/PS does not increased with the increasing of coating layers. In our case, TiO_2/PS particles with 2 coating layers exhibit the optimum photocatalytic activity. The reason can be explained that TiO_2 particles on the surface PS particles coated 2 layers, have better distribution and larger surface area. The large surface area is an important contribution to its excellent activity in that it can absorb more oxygen and molecular water [23].

Table 1 Degradation rate of methyl orange by using TiO_2/PS (1–8 layers) as photocatalyst

Number of coating layers	1	2	3	4	5	6	7	8
Degradation rate of methyl orange	65%	83%	79%	75%	73%	76%	74%	75%

The photocatalytic activity of TiO_2/PS (calcined at 260 °C) and hollow TiO_2 spheres (calcined at 450 °C) with 8 coating layers was determined by the degradation rate of methyl orange which is shown in Fig. 9. We can see that the photocatalytic activity of hollow TiO_2 spheres is higher than that of TiO_2/PS.

It can be explained by the following two main factors: the increasing of high crystallinity and surface area. With increasing calcination temperature, we can obtain high crystalline TiO_2 (as shown in Fig. 8). In other words, the

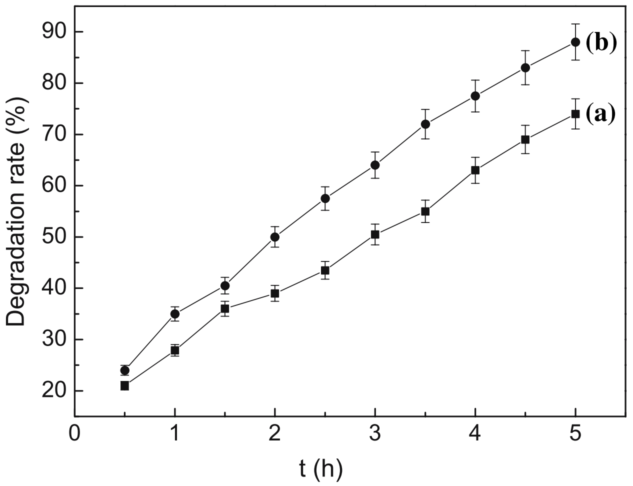

Fig. 9 Degradation rate of methyl orange with reaction time between TiO_2/PS (**a**) and hollow TiO_2 spheres (**b**)

photo-catalytic activity increases due to the decrease of amorphous phase which has non photo-catalytic activity. Moreover, hollow TiO_2 spheres should exhibit larger surface area owing to special structure, and then have higher photocatalytic activity. In addition, surface state and electron structure of TiO_2 and PS particles are difference at different calcination temperatures, which can affect the photo-catalytic activity. Further work will is proceeding in our laboratory.

Conclusion

In this paper, we have prepared pure rutile (TiO_2) nanostructured materials at low temperature from $TiCl_4$ aqueous solution using simple method and simple facilities. Nanostructured TiO_2/PS particles have been obtained by layer-by-layer assembly technique. The experimental results showed that pure rutile-TiO_2 coatings were synthesized at 100 °C. On the surface of PS particles, sphere-type TiO_2 coatings displayed uniform shape and had a narrow size distribution. The amount of TO_2 (wt%) shell increased with the adding of coating layers. Hollow balls of TiO_2 were obtained by calcination at 450 °C. TiO_2/PS with 2 coating layers showed the optimum photocatalytic activity. The photocatalytic activity of hollow TiO_2 spheres is higher than that of TiO_2/PS. The rutile (TiO_2) nanostructured materials obtained by this method will be possibly potential applications for water purification photocatalysis.

Acknowledgement This work was supported by a grant from the National Natural Science Foundation of China (50342016).

References

1. Yang J, Mei S, Ferreira JMF, Norby P, Quaresma S (2005) J Collid Interface Sci 283:102
2. Chen Y-F, Lee C-Y, Yeng M-Y, Chiu H-T (2003) J Cryst Growth 247:364
3. Hoffmann MR, Martin ST, Choi W, Bahnemann DW (1995) Chem Rev 95:9
4. Yin S, Hasegawa H, Maeda D, Ishitsuka M, Sato T (2004) J Photochem Photobio 163:1
5. Kim KJ, Benksten KD, Van De Lagemaat J, Frank AJ (2002) J Chem Mater 14:1042
6. Tao N, Zhao J, Guo Y, Jiang Y, Ding X, Wang Z (2004) Mater Chem Phys 84:58
7. Yang Q, Xie C, Xu Z, Gao Z, Du Y (2005) J Phys Chem B 109:5554
8. Wang W, Gu B, Liang L, Hamilton AW, Wesolowski DJ (2004) J Phys Chem B 108:14789
9. Wu M, Lin G, Chen D, Wang G, He D, Feng S, Xu R (2002) Mater Chem 14:1974
10. Navrotsky A (2003) Geochem Trans 4:34
11. Park HK, Kim WDK, Kim CH (1997) J Am Ceram Soc 80:743
12. Li Y, Fan Y, Chen Y (2002) J Mater.Chem 12:1387
13. Samuel V, Pasricha R, Ravi V (2005) Ceram Int 31:555
14. Li Y-L, Ishigaki T (2004) J Phys Chem B 108:15536
15. Ito S, Takeuchi T, Katayama T, Sugiyama M et al. (2003) Chem Mater 15:2824
16. Eiden S, Maret G. (2002) J Colloid Interf Sci 250:281
17. Boccaccini AR, Karapappas P, Marijuan JM (2004) J Mater Sci 39:851
18. Nishino J, Teekateerawej S, Nosaka Y (2003) J Mater Sci Letters 22:1007
19. Zan L, Peng Z-H, Xia Y-L, Huang L (2004) J Mater Sci 39:761
20. Eiden S, Maret G (2002) J Collid Interf Sci 250:281
21. Yin S, (2002) Mater Chem Phys 75:76
22. Li Y, Lee N-H, Hwang D-S, Song JS, Lee EG, Kim S-J (2004) Langmuir 20:10838
23. Yang Q, Xi C, Xu Z, Ga Z, Du Y (2005) J Phys Chem B 109:5554